Journal of
Composites Science

MDPI

Article

Mechanical Response and Processability of Wet-Laid Recycled Carbon Fiber PE, PA66 and PET Thermoplastic Composites

Uday Vaidya [1,2,3,*], Mark Janney [4], Keith Graham [4], Hicham Ghossein [1] and Merlin Theodore [2,5]

[1] Tickle College of Engineering, University of Tennessee, 1512 Middle Drive, Knoxville, TN 37996, USA; hghossei@utk.edu
[2] Manufacturing Sciences Division (MSD), Oak Ridge National Laboratory (ORNL), 2350 Cherahala Blvd, Oak Ridge, TN 37932, USA; theodorem@ornl.gov
[3] The Institute for Advanced Composites Manufacturing Innovation, IACMI-The Composites Institute, 2370 Cherahala Blvd, Knoxville, TN 37932, USA
[4] Carbon Conversions, Lake City, SC 29560, USA; mjanney52@gmail.com (M.J.); kgraham@carbonconversions.com (K.G.)
[5] Carbon Fiber Technology Facility, Oak Ridge National Laboratory, Oak Ridge, TN 37830, USA
* Correspondence: uvaidya@utk.edu

Abstract: The interest in recycled carbon fiber (rCF) is growing rapidly and the supply chain for these materials is gradually being established. However, the processing routes, material intermediates and properties of rCF composites are less understood for designers to adopt them into practice. This paper provides a practical pathway for rCFs in conjunction with low cost and, for the most part, commodity thermoplastic resins, namely polyethylene (PE), polyamide 66 (PA66) and polyethylene terephthalate (PET). Industrially relevant wet-laid (WL) process routes have been adopted to produce mats using two variants of WL mats, namely (a) high speed wet-laid inclined wire to produce broad good 'roll' forms and (b) 3DEP^{TM} process patented by Materials Innovation Technologies (MIT)-recycled carbon fiber (RCF), now Carbon Conversions, which involves mixing fibers and water and depositing the fibers on a water-immersed mold. These are referred to as 'sheet' forms. The produced mats were evaluated for their processing into composites as 'fully consolidated mats' and 'non-consolidated' as-produced mats. Comprehensive mechanical data in terms of tensile strength, tensile modulus and impact toughness for rCF C/PE, C/PA66 and C/PET are presented. The work is of high value to sustainable composite designers and modelers.

Keywords: recycled carbon fiber; thermoplastics; wet-laid processing; compression molding

Citation: Vaidya, U.; Janney, M.; Graham, K.; Ghossein, H.; Theodore, M. Mechanical Response and Processability of Wet-Laid Recycled Carbon Fiber PE, PA66 and PET Thermoplastic Composites. *J. Compos. Sci.* **2022**, *6*, 198. https://doi.org/10.3390/jcs6070198

Academic Editor: Jiadeng Zhu

Received: 19 June 2022
Accepted: 5 July 2022
Published: 7 July 2022

1. Introduction

Discontinuous carbon fibers have a number of advantages, such as (a) fiber aspect ratio can be greater than critical fiber length, hence, superior mechanical properties can be realized; (b) higher drapeability offered due to fiber movement during processes, such as compression and thermo-stamping; (c) ability to hybridize fiber lengths and types; and (d) lower cost, since secondary weaving and braiding are not necessary. Traditional processes, such as injection molding and extrusion, result in significant fiber length attrition due to friction and interaction with the screw with the material. Wet-laid (WL) processing offers a low-energy alternative to traditional processes, such as weaving and/or stitch bonding, producing mats in desired fiber-matrix weight fraction. Both reinforcing fibers and resin fibers (resin in fiber form) are mixed in desired weight proportion in water (with dispersant and flocculent) and mixed till the material assumes a homogenous form. The water is drained rapidly from the fiber bulk, resulting in a well-dispersed fiber-polymer mat.

Two types of industrially relevant WL mat process routes have been investigated in this work, namely—(a) high speed wet-laid line to produce broad good 'roll' forms and (b) 3DEP^{TM} process patented by Carbon Conversions, mixing fibers and water, and

depositing on a water-immersed mold. The underlying hypothesis is that the high-speed WL process would yield preferred fiber alignment in the 'roll' direction, while the 3DEP™ would produce randomized fiber orientation. This work reports mechanical properties of WL-processed rCF mat composites in conjunction with commodity thermoplastics, namely polyethylene (PE) and polyethylene terephthalate (PET) and engineering thermoplastic polyamide (PA66). There is no work, to our knowledge, that quantifies the mechanical performance of rCF WL mat composites, while such information would be valuable to a designer and modeler(s).

2. Literature Review

With increased emphasis on circular economy, rCFs are finding use in applications, such as automotive, sporting goods and industrial parts [1–5]. The processes used to obtain rCF are pyrolysis and solvolysis of out-of-date prepregs and end-of-life CF intensive parts. Other sources include manufacturing scrap, edge trims and waste from textile processes. Carbon Conversions specializes in pyrolysis-based recovery of CFs [6], the primary focus of this effort. Several efforts have emphasized the importance of processing discontinuous carbon fiber thermoplastic composites [7–9].

Thomason [10] and Vaidya [11] illustrated the importance of fiber aspect ratio of discontinuous fibers. Polyamide (PA), polyethylene (PE) and polyethylene terephthalate (PE) are of continued interest as thermoplastic matrices in reinforced composites due to their recyclability and superior mechanical properties [12–14].

The WL process is promising in terms of fiber length retention. Hemamalini and Dev [15] discussed that WL is an emerging technique to produce nonwovens using short natural cellulosic fibers and synthetic fibers and their blends. The steps involved in wet laying are dispersion, deposition and consolidation. Uniform dispersion is the key to attain defect-free nonwovens in web laying. WL processing is like the papermaking process with differences in fiber length and density of the fibers [16,17]. The quality of the dispersion depends on material parameters, such as fiber length, surfactant, source of the fibers, linear density of the fibers and machine parameters, such as dispersion time and mechanical agitation.

There are only limited studies with WL and thermoplastic polymers in conjunction with high-performance CFs [17]. Product opportunities for automotive and aerospace can expand using WL intermediates. This work considers WL rCFs in conjunction with commodity thermoplastics, such as PP and PET, as well as engineering thermoplastics, such as PA66. Yan et al. [18] investigated process parameters of WL rCF-reinforced thermoplastic (CFRTP) nonwoven mats. They used response surface methodology to optimize the heat-molding compression parameters in terms of temperature, pressure and time, respectively. They also reported that CFRTP comprising 30 wt% CF fiber length of 6 mm provided the highest tensile strength. Ghossein et al. [19] evaluated the mechanical behavior of WL-CF mats in conjunction with the microstructure predicted through Object-Oriented Finite Element Analysis (OOF). The authors used novel mixing methods to reduce time to create optimal mats. Barnett et al. [20] created CF-PPS WL mats, similar to organosheets used in automotive production. Erland et al. [21] investigated the re-manufacture and repairability of thick-section poly(ether ether ketone) PEEK CFRTPs. They reported results on C/PEEK tested under three-point bend loaded to fracture before being re-heated, re-pressed and re-tested. Their study showed that C/PEEK composites could be repaired with minimal loss of mechanical performance, even when significant fracture occurs. They attained a flexural modulus of 80 GPa and a maximum bending stress of 900 MPa. Brahma et al. [22] investigated discontinuous WL CF mats and compared them to liquid-molded PA6. There was roughly a 10–13% increase in its tensile strength, modulus and impact strength properties at 30 and 40% weight fractions and almost a 120% increase at 50% weight fraction. Yeole et al. [23] studied the effects of dispersant and flocculent in glass fiber WL thermoplastic composites. Kore et al. [24] hybridized bamboo fibers with carbon fiber mats with the WL process and reported the property bounds.

There are presently no systematic guidelines of using rCF in composite products. This paper attempts to address this gap, and addresses commodity and engineering thermoplastics with rCFs to provide a comprehensive understanding of lower- and upper-bound properties with these materials. The work is of high relevance to sustainable composite designers and end users.

3. Materials and Methods

Two WL-processing approaches were considered in this study. Nonwoven rCF-thermoplastic mats were produced (a) in a WL machine capable of producing 'roll' forms; and (b) 3DEP^{TM} process where rCF mats were deposited as a 'sheet' in a water tank. Throughout this manuscript these variants are referred to as 'roll' and 'sheet' forms, respectively.

The 'roll' mats were produced in 1.2 m (48") wide rolls, while the 'sheets' were produced as 3DEP^{TM} mats using a water-based deposition on a screen tool. A 'sheet' was typically 350 mm × 350 mm WL mat.

'Sheet': Carbon Conversions developed an innovative method for making WL fiber preforms [5]. The 3DEP^{TM} process lends itself to converting loose recycled fibers into nonwoven carbon fiber mats. The 3DEP^{TM} process uses advanced slurry molding process for creating nonwoven rCF preforms. 3DEP^{TM} produces homogeneous fiber distribution within the mat with consistent areal weight and acceptable dimensional tolerance. In this work 3DEP^{TM} was used to produce WL rCF mats. rCF obtained from pyrolysis of T800 prepreg were used. The recycled fiber had nominal 12.7 mm fiber length and 8–10 mm diameter.

'Roll': Carbon Conversions produces continuous, WL, nonwoven fabrics on a 1.2 m wide RotoFormer machine (Allimand Interweb, Inc., Glen Falls, NY, USA). Compositions include chopped carbon fiber and blends of carbon fiber with thermoplastic polymer staple fibers. Areal density can range from 100 to 500 g/m^2 (gsm). Areal density coefficient of variation (COV) is typically <3%. After forming, the web is sent through a continuous dryer and then bound onto 50–200 m rolls. rCF mats were processed via WL with three resin systems: PE, PA66 and PET, respectively. The molecular weights are as follows: PET—25,000 g/mol, PE—30,000 g/mol and PA66—25,000 g/mol. The tensile modulus of neat (unreinforced) PET is 2.8 GPa, PE is 0.9 GPa and PA66 is 3.2 GPa, respectively.

The C/PET and C/PA66 were processable at 500 F due to their higher melting point, while PE was processed at 250 F since PE melts at a lower temperature. The work was conducted in two batches referred to as *Batch 1* and *Batch 2.* The lessons from *Batch 1* were applied in producing *Batch 2* mats. Table 1 summarizes the rCF mats designed for the 'roll' and 'sheet' forms under *Batch 1*. *Batch 2* mats are discussed later. Composite panels were made from the WL mats using compression-molding process with the process conditions identified in the table.

Table 1. Sample variants, preform type and processing conditions for *Batch 1* mats.

Sample Variant **	Preform Type	Processing Notes ˆ
PA66/CF/68/30	Sheets	Tool at 500 F and 1000 psi
PA66/CF/78/20	Sheets	Tool at 500 F and 1000 psi
PA66/CF/88/10	Sheets	Tool at 500 F and 1000 psi
PA66/CF/77/20	Roll	Tool at 500 F and 1000 psi
PE/CF/78/20	Roll	Tool at 250 F and 1000 psi
PA66/CF/77/20	Roll	Tool at 509 F and 1000 psi
PA66/CF/78/20	Dried Sheets	Tool at 509 F and 1000 psi
PE/CF/77/20	Roll	Tool at 265 F and 1000 psi
PE/CF/77/20	Roll	
PET/CF/77/20	Sheets	Tool at 500 F and 1000 psi

ˆ All plates were compression molded; ** e.g., nomenclature PA66/CF/68/30 means, 68% resin, 30% carbon fiber by weight.

4. Results and Discussion

4.1. Partial and Fully Consolidated Panels

Compression molding was used to produce partially and fully consolidated panels as illustrated in Figure 1a–f. Five (5) layers of 300 mm × 300 mm preforms were compression molded in a matched metal tool. For C/PA66, the press platens were heated to a temperature of 500 °F at 6.895 MPa (1000 psi). In a few cases, the tool temperature was held at 250–265 °F. The hold time was approximately 20 min at temperature. The tool was cooled to room temperature. In some cases, slight discoloration was noted along the edges of the panel—12 mm wide band along the four edges.

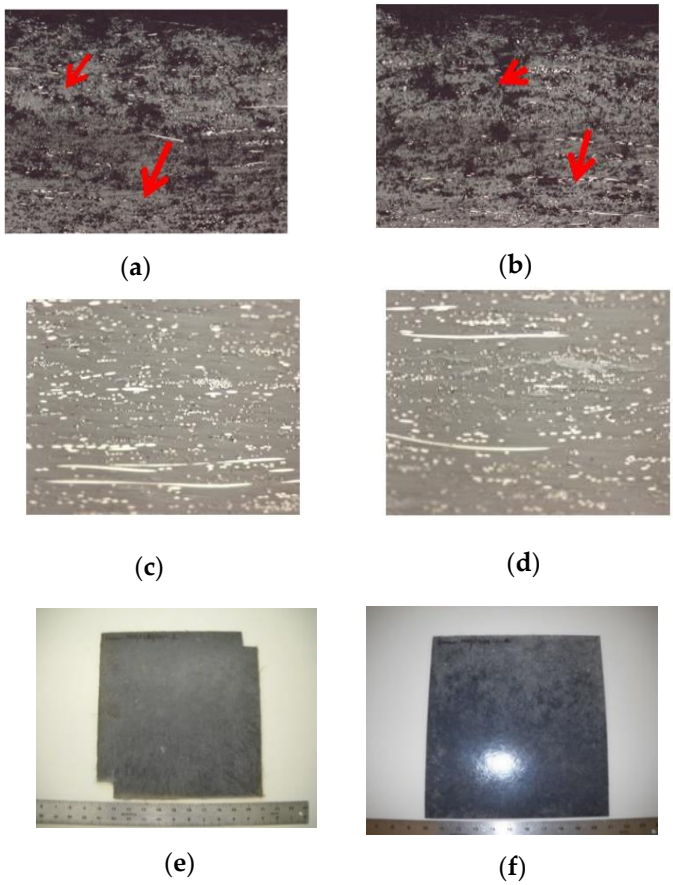

Figure 1. Effect of consolidation; (**a**) PA66/CF/68/30, 5 layers of preform (less-consolidated panel); (**b**) PA66/CF/88/10, 5 layers of preform (less-consolidated panel). Arrows point to representative voids in both (**a**,**b**); (**c**) PA66/CF/68/30, 5 layers of preform (well-consolidated panel); (**d**) PA66/CF/88/10, 5 layers of preform (well-consolidated panel); (**e**) PA66/CF/68/30 less-consolidated panel, the PA66/CF/88/10 was similar in look; (**f**) PA66/CF/68/30 well-consolidated panel, the PA66/CF/88/10 was similar in look; Panel size 275 mm × 275 mm.

The C/PE and C/PET panels were produced in a similar manner to C/PA66. Two panels of PE-CF-78-20 roll were processed as three layers of preforms were compression molded in a 300 × 300 mm matched metal tool. The tool was heated to a temperature of 250 °F (for C/PE) and 500 °F (for C/PET) at 6.895 MPa (1000 psi). The hold time was approximately 20 min at these temperatures. The tool was cooled to room temperature.

4.2. 'Roll' versus 'Sheet' Forms

Preform "sheets" and "roll" forms were evaluated in similar weight fraction and resin type(s). For example, 'sheet(s)' PA66-CF-68-30 and PA66-CF-78-20 and 'roll' PA66-CF-77-20 (e.g., PA66-CF-77-20 means 77 wt% PA66 and 20 wt% CF) were evaluated and compared. Qualitatively, the 'roll' form processed under similar conditions consolidated better (less

voids) than 'sheets'. Figure 2 illustrates a representative 'roll' and 'sheet' form composite panel. Moisture analysis revealed that the 'roll' form had less moisture content. The material was dried before consolidation. Parallel edge coupons were tabbed and tested in two (2) directions 'along' and 'across' the machine direction. The direction was more relevant in the 'roll' due to preferential fiber orientation along the warp (machine) direction.

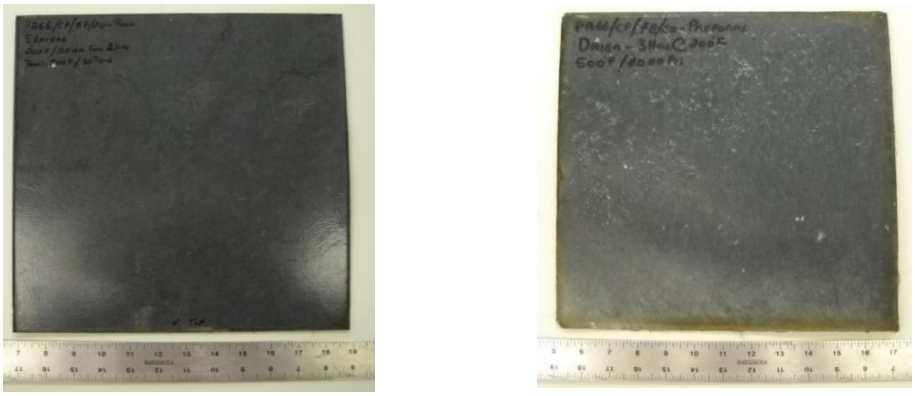

(**a**) (**b**)

Figure 2. 'Roll' and 'Sheet' form panel; (**a**) 'Roll' form panel—optimal compression-molded C/PA66 panel from WL mats; (**b**) panel produced from WL PA66-CF mats in 'sheet' form. Panel size 300 × 300 mm^2.

4.3. Moisture Analysis

Moisture analysis was conducted to determine moisture content in the preform 'sheets and 'roll'. Percentage moisture was determined by weight analysis. The samples studied were PA66-CF-78-20 preform 'sheets' and PA66-CF-77-20 preform "roll". The materials were dried at 250 °F for 8 h. Table 2 illustrates the moisture percent in the 'sheet' versus 'roll' preform. The 'sheet' exhibited an average moisture content of 3% while the 'roll' exhibited average moisture of 1.68%, about 45% lower than the 'sheet'.

Table 2. Moisture analysis of WL PA66-CF 'sheet' and 'roll' forms.

Sample ID	Wet Sample	Dry Sample	Moisture Content	Moisture %
PA66/CF/78/20/Preform Sheets-1	2.6057	2.53	0.08	3.03
PA66/CF/78/20/Preform Sheets-2	2.8037	2.72	0.08	3.00
PA66/CF/77/20/Preform Roll-1	3.7176	3.65	0.06	1.70
PA66/CF/77/20/Preform Roll-2	3.5691	3.51	0.06	1.66

Tension samples were cut from the consolidated 300 × 300 mm^2 plate. Flat-wise tabs were used for the tension samples (25.4 mm wide and 200 mm length). Some dog bone samples were also tested in a couple of variants to observe the effect of sample shape and size of final properties. Strength and modulus were determined for three specimens each, 'along' and 'across' the fiber directions at a rate 2 mm/min. The modulus was determined with an extensometer (0.2% to 1 % strain).

4.4. Batch 1 Results

Tables 3 and 4 summarize the tensile modulus and strength for composites made with C/PA66 'sheets' versus 'roll', respectively. It is seen that the C/PA66 'roll' had 67% higher

average tensile strength (108 MPa ('sheet') versus 187.73 MPa ('roll')) and 72% higher average modulus (10 GPa ('sheet') versus 16.5 GPa ('roll')). The high values for the 'roll' can be attributed to the preferential fiber alignment in the 'roll' direction while the 'sheet' exhibits quasi-isotropic/random orientation. There was no statistical difference in the tensile strength and modulus between the flat edge specimens compared to the dog bone specimen geometry as shown in Table 5.

The 30 wt% C/PE 'roll' specimens exhibited an average tensile strength of 45 MPa and tensile modulus of 6.5 GPa. These were approximately half that of the 30 wt% C/PA66 composites. The C/PE was only tested (available) in the 'roll' direction.

Table 3. Tensile modulus and strength of C/PA66 (preform 'Sheets').

Type	Sample ID	Direction	Average Modulus (GPa)	Average Modulus 10^6 (psi)	Average Strength (MPa)	Average Strength 10^3 (psi)	Density (g/cc)	Specific Strength	Specific Modulus
Flat Tension Coupons	PA66-CF-68-30	1	10.01	1.45	108.00	15.66	1.24	8.07	87.09
	PA66-CF-68-30	2	9.95	1.44	103.49	15.01	1.24	8.02	83.46
	PA66-CF-78-20	1	10.01	1.45	108.00	15.66	1.21	8.27	89.25
	PA66-CF-78-20	2	9.98	1.45	105.74	15.34	1.21	8.25	87.39
	PA66-CF-88-10	1	9.99	1.45	106.49	15.44	1.18	8.46	90.25
	PA66-CF-88-10	2	9.98	1.45	105.74	15.34	1.18	8.46	89.61
Dog Bone	PA66-CF-78-20	1	9.98	1.45	105.99	15.37	1.21	8.25	87.60

Table 4. Tensile modulus and strength of C/PA66 (preform 'Roll').

Type	Sample ID	Avg. Modulus (GPa)	Avg. Modulus 10^6 (psi)	Avg. Strength (MPa)	Avg. Strength 10^3 (psi)	Density (g/cc)	Specific Strength	Specific Modulus
Flat Samples	PA66-CF-77-20 *	15.32	2.22	187.72	27.23	1.21	12.66	155.14
	PA66-CF-77-20 ^	17.07	2.48	178.16	25.84	1.21	14.11	147.24
Dog Bone	PA66-CF-77-20 ^	16.20	2.35	182.94	26.53	1.21	13.38	151.19

* 2 direction, ^ 1direction.

Table 5. Tensile modulus and strength—C/PE (preform Roll).

Sample Type	Sample ID	Avg. Modulus (GPa)	Avg. Modulus 10^6 (psi)	Avg. Strength (MPa)	Avg. Strength 10^3 (psi)	Density	Specific Modulus	Specific Strength
Flat Samples	PE-CF-78-20	5.19	0.75	40.39	5.86	1.03	5.04	39.21
Dog Bone	PE-CF-78-20	4.21	0.61	47.72	6.92	1.03	4.09	46.33

4.5. Batch 2 Results—Tensile Modulus and Tensile Strength

Based on the results from *Batch 1*, a controlled set of preforms was prepared with approximately 20 wt% CF for PA66, PE and PET, respectively. Composite plates were produced in two configurations, namely, 'no cross-stack' and 'cross-stack', respectively. The rationale for the two configurations was to evaluate if the preferential fiber orientation in the 'roll' influenced the stacking sequence.

Tables 6–8 summarize the results from these materials. The trend of the 'roll' form of higher values than the 'sheet' forms was similar to that in Batch 1. The 'roll' form had 88% higher strength and 137% higher modulus compared to the 'sheet' form. This indicates the influence of significant fiber orientation in the 'roll' form. The effect of drying the mats in *Batch 2* had a marked influence in the 'sheet' form. Drying improved the tensile strength and modulus by an average factor of two or greater.

Table 6. Tensile modulus and strength of PA66-CF (preform 'Roll').

Sample ID	Preform Type	Stacking Sequence	Direction	Tensile Modulus	Tensile Strength
				(GPa)	(MPa)
PA66-CF-77-20-CS	Roll	Cross Stack	1	19.98	257.70
PA66-CF-77-20-CS	Roll	Cross Sack	2	15.16	217.34
PA66-CF-77-20-NCS	Roll	No Cross Stack	1	20.57	242.06
PA66-CF-77-20-NCS	Roll	No Cross Stack	2	16.92	248.29

Table 7. Tensile modulus and strength of PA66-CF (preform 'Sheet').

Sample ID	Preform Type	Stacking Sequence	Direction	Tensile Modulus	Tensile Strength
				(GPa)	(MPa)
PA66-CF-78-20-Predried	Sheets	N/A	1	10.66	169.95
PA66-CF-78-20-Predried	Sheets	N/A	2	6.39	84.31

Table 8. Tensile modulus and strength—PE-CF (preform 'Roll').

Sample ID	Preform Type	Stacking Sequence	Direction	Tensile Modulus	Tensile Strength
				(GPa)	(MPa)
PE-CF-77-20-CS	Roll	Cross Stack	1	5.50	53.74
PE-CF-77-20-CS	Roll	Cross Stack	2	5.57	52.43
PE-CF-77-20-NCS	Roll	No Cross Stack	1	4.20	39.41
PE-CF-77-20-NCS	Roll	No Cross Stack	2	6.97	66.48
PE-CF-77-20-MIT	Roll	N/A	1	5.80	53.27
PE-CF-77-20-MIT	Roll	N/A	2	7.57	75.11

Batch 2 of the PE/CF panels was processed at a higher temperature than Batch 1 (260 °F instead of 245 °F). Increasing the processing temperature increased the tensile strength marginally. The cross-stack panel exhibits similar properties in both the directions while the no-cross stack exhibits a difference in properties in the two directions as shown in Table 9.

Table 9. Tensile modulus and strength—C/PET (preform 'Roll').

Sample ID	Preform Type	Stacking Sequence	Direction	Tensile Modulus	Tensile Strength
				(GPa)	(MPa)
PET-CF-77-20	Sheets	N/A	1	17.35	243.84
PET-CF-77-20	Sheets	N/A	2	17.41	271.19

C/PET sheet preforms were processed at 500 F and 100 psi. These exhibit excellent tensile modulus and strength and are comparable to the C/PA66 samples. Table 10 compares

the density of the mats for different weight fractions for C/PA66, C/PET and C/PE, respectively. The C/PA66 composite density ranged from 1.18 and 1.21 to 1.24 g/cc for 10%, 20% and 30 wt%, respectively. The C/PE was 1.03 and C/PET 1.42 g/cc for 20 wt%, respectively. The densest of the materials was C/PET. Table 11 summarizes typical (standard) materials, such as aluminum, ABS and long glass fiber thermoplastics, for comparison to the carbon fiber mats in terms of the density, strength and modulus, respectively. Table 12 provides a detailed summary of all material variants studied in this work C/PA66, C/PE and C/PET for 'roll' and 'sheet' forms in no-stack and cross-stack configurations, where applicable. The data are summarized in terms of density, strength, modulus, specific strength and specific modulus.

Table 10. Density of the rCF thermoplastic variants.

Sample Variants	Fiber	Resin	Fiber Density	Resin Density	Fiber Volume	Resin Volume	Composite Density
	Weight %	Weight %	g/cm^3	g/cm^3	Fraction	Fraction	g/cm^3
Carbon/PA66	10	90	1.50	1.15	0.078	0.922	1.18
Carbon/PA66	20	80	1.50	1.15	0.161	0.839	1.21
Carbon/PA66	30	70	1.50	1.15	0.247	0.753	1.24
Carbon/Polyethylene	20	80	1.50	0.955	0.137	0.863	1.03
Carbon/PET	20	80	1.50	1.40	0.189	0.811	1.42

Table 11. Specific strength and specific modulus of other engineering materials.

Sample ID	Density	Young's Modulus	Tensile Strength	Specific Modulus	Specific Strength
	(g/cm^3)	(GPa)	(MPa)	(GPa/(g/cm^3))	(MPa/(g/cm^3))
Aluminum	2.70	70.00	570.00	25.93	211.11
ABS (Impact Grade) Min	1.02	1.40	28.00	1.37	27.45
ABS (Impact Grade) Max	1.20	2.80	138.00	2.33	115.00
Glass-PP-40-60	1.21	8.27	80.00	6.83	66.12

Table 12. Comprehensive summary of tensile strength, tensile modulus, specific strength and specific modulus for all rCF variants in this study. The effect of stacking sequence and 'roll' versus 'sheet' form are included.

Sample ID	Preform Type	Stacking Sequence	Direction	Tensile Modulus	Tensile Strength	Density	Specific Modulus	Specific Strength
				(GPa)	(MPa)	g/cm^3	((GPa)/(g/cm^3))	((MPa)/(g/cm^3))
PA66-CF-77-20-CS	Roll	Cross Stack	1	19.98	257.70	1.21	16.51	212.97
PA66-CF-77-20-CS	Roll	Cross Stack	2	15.16	217.34	1.21	12.53	179.62
PA66-CF-77-20-NCS	Roll	No Cross Stack	1	20.57	242.06	1.21	17.00	200.05
PA66-CF-77-20-NCS	Roll	No Cross Stack	2	16.92	248.29	1.21	13.98	205.20
PA66-CF-78-20-Predried	Sheets	N/A	1	10.66	169.95	1.21	8.81	140.45
PA66-CF-78-20-Predried	Sheets	N/A	2	6.39	84.31	1.21	5.28	69.68
PE-CF-77-20-CS	Roll	Cross Stack	1	5.50	53.74	1.03	5.34	52.17
PE-CF-77-20-CS	Roll	Cross Stack	2	5.57	52.43	1.03	5.40	50.90
PE-CF-77-20-NCS	Roll	No Cross Stack	1	4.20	39.41	1.03	4.08	38.27
PE-CF-77-20-NCS	Roll	No Cross Stack	2	6.97	66.48	1.03	6.76	64.54
PE-CF-77-20-MIT	Roll	N/A	1	5.80	53.27	1.03	5.63	51.72
PE-CF-77-20-MIT	Roll	N/A	2	7.57	75.11	1.03	7.35	72.92
PET-CF-77-20	Sheets	N/A	1	17.35	243.84	1.42	12.22	171.72
PET-CF-77-20	Sheets	N/A	2	17.41	271.19	1.42	12.26	190.98

4.6. Low-Velocity Impact Testing

The specimens were subjected to drop tower impact on a Dynatup 8250 under clamped plates 100 × 100 mm with drop height impact for two energy levels (5 J and 15 J) (or drop heights), referred to as 'low-energy 5 J' and 'high-energy 15 J' impact. Tables 13 and 14 summarized the impact data for all variants tested for drop weight impact. Figures 3 and 4 compares the normalized load and normalized energy for variants of 20 wt% carbon fiber in each of C/PA66, C/PET and C/PE for no-stack versus cross-stack, where applicable.

Table 13. Low-velocity impact results at low-impact energy (5 J).

Variant	Thickness (mm)	Max Load (kN)	Energy at Max Load (Joule)	Normalized Max Load (kN/mm)	Normalized Energy (Joule/mm)
MIT-C/PE/77/20	2.50	1.83	7.10	0.73	2.84
C/PE/77/20 Cross Stack	2.85	1.84	7.17	0.65	2.52
C/PE/77/20 No Cross Stack	2.69	1.59	6.89	0.59	2.56
C/PA66/77/20 Cross Stack	2.25	1.46	7.45	0.65	3.31
C/PA66/77/20 No Cross Stack	2.03	1.15	7.15	0.57	3.52
C/PET/77/20	2.78	2.08	7.26	0.75	2.61

Table 14. Low-velocity impact results at higher impact energy (15 J).

Sample Variant	Sample Thickness (mm)	Max Load (kN)	Energy at Max Load (Joule)	Normalized Max Load (kN/mm)	Normalized Energy (Joule/mm)
C/PE/77/20	2.46	1.84	11.64	0.75	6.33
C/PE/77/20 Cross Stack	2.77	2.03	12.41	0.73	6.11
C/PE/77/20 No Cross Stack	2.56	1.63	10.83	0.64	6.64
C/PA66/77/20 Cross Stack	1.81	1.66	3.30	0.92	1.99
C/PA66/77/20 No Cross Stack	2.13	1.46	4.91	0.69	3.36
C/PET/77/20	2.69	2.17	6.63	0.81	3.06

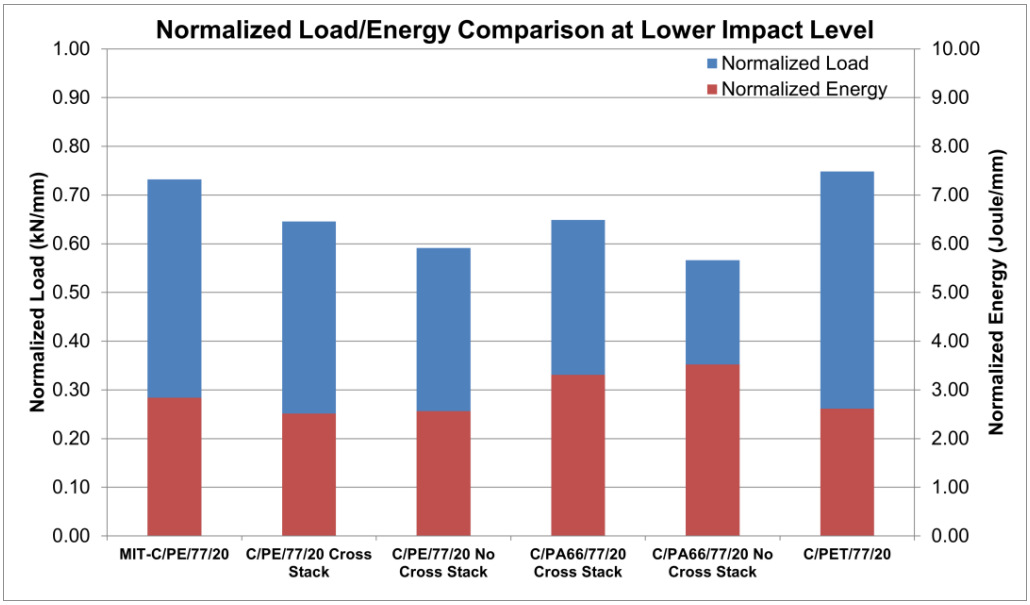

Figure 3. Comparison at normalized load and normalized energy for rCF variants at 5 J impact energy.

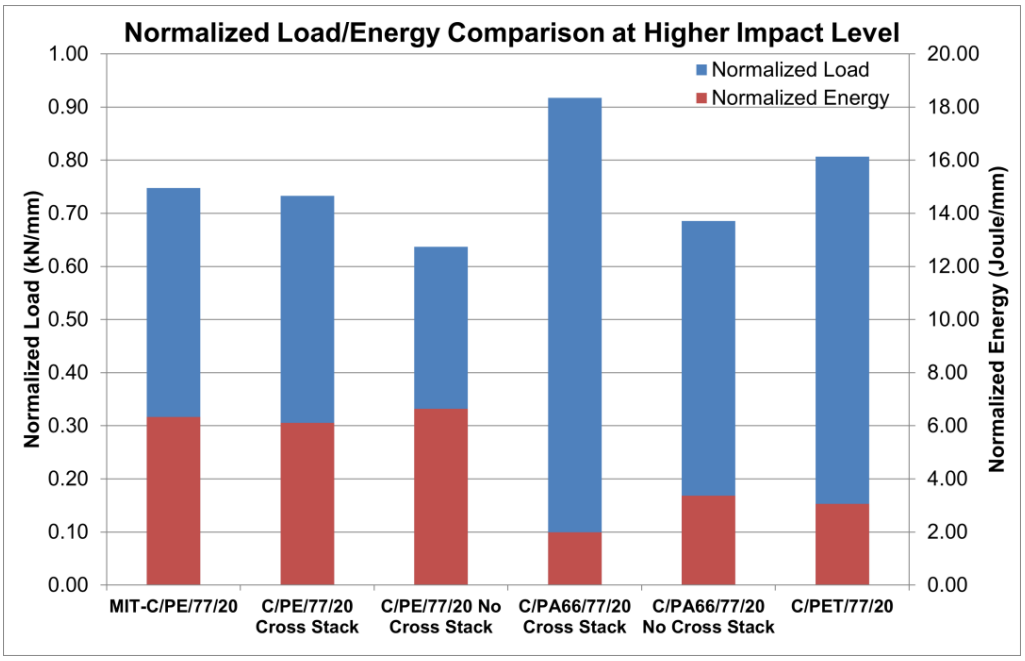

Figure 4. Comparison normalized load and normalized energy for rCF variants at 15 J impact energy.

At lower energy, the highest peak loads attained were from C/PE and C/PET, respectively. In both these systems, once the peak on the force–time curve was attained, there was penetration of the impactor through the thickness, and the unloading was, hence, sudden. While the normalized energy was highest for C/PA66, both no-stack and cross-stack compared to the rest. This suggests that C/PA66-exhibited-energy absorption occurs both in the loading and unloading phase. There is no penetration of the indenter for C/PA66.

For higher energy impact, C/PA66 and C/PET exhibited the highest normalized load bearing for the cross-stack. The highest energy absorbed was noted for all C/PE variants, regardless of no-stack or cross-stack.

The effect of stacking was less pronounced in all the impact tested samples. This may be due to localized transverse impact and only limited contact area between the impactor and the specimen. Cross-stack or no-stack is more of a function for in-plane loading. The peak load in case of drop weight impact is the onset at which the unloading phase begins. Energy absorption continues into the unloading phase for damage-tolerant materials. Overall, the PA66 offered higher damage tolerance in terms of energy absorption, for both low- and high-energy impact.

5. Discussion

Figures 5–7 provide a comprehensive visual of all tests conducted for C/PA66, C/PE and C/PET, respectively. Where applicable, the no-stack versus cross-stack has been reported. The overall tensile strength of 'roll' form of C/PA65 ranged from 217 to 248 MPa and tensile modulus of 15–20 GPa, respectively. The differences between cross-stack and no-stack are not very definitive, indicating fiber entanglement occurs in discontinuous fibers, masking the distinct effect of fiber orientation. In some cases, modulus and strength for cross-stack were lower by 12.5% compared to no-stack.

For 77 wt% C/PET (i.e., 23% CF), the highest values of strength ranged from 243 to 271 MPa and modulus 16–17 GPa for the 'sheet' form. For the 'roll' form, there was a distinct difference in the cross-stack versus no-stack, or high anisotropy. The values ranged from 128 to 170 MPa and modulus of 5–10 GPa, much lower than other variants. Further, the fiber content in these was only 15 wt%, unlike the others, which were >20 wt% carbon fiber. It may also be noted for the no-stack roll form, when a high degree of fiber orientation

in the machine direction occurs, the strength and modulus are high, i.e., 256 MPa and 16 GPa, respectively.

The 77 wt% C/PE (i.e., ~20 wt% carbon fiber) exhibited the lowest values of all. For cross-stack, the average modulus was 53 MPa and average strength was 5.5 GPa, similar in both directions for cross-stack. For the no-cross stack, significant anisotropy was observed at 39 and 66 MPa and 4 and 6 GPa modulus.

Figure 8 considers a long fiber thermoplastic C/PPS with 40 wt% 25 mm (1″) fiber length, which has strength of 175 MPa and modulus 25 GPa. Although this is not a one-to-one comparison, both C/PA66 and C/PET rCF mat composites have much higher modulus (by 37 %), higher than LFT C/PPS. The strength of C/PPS was 25% higher, the C/PA66 rCF mats providing the closest to the LFT values.

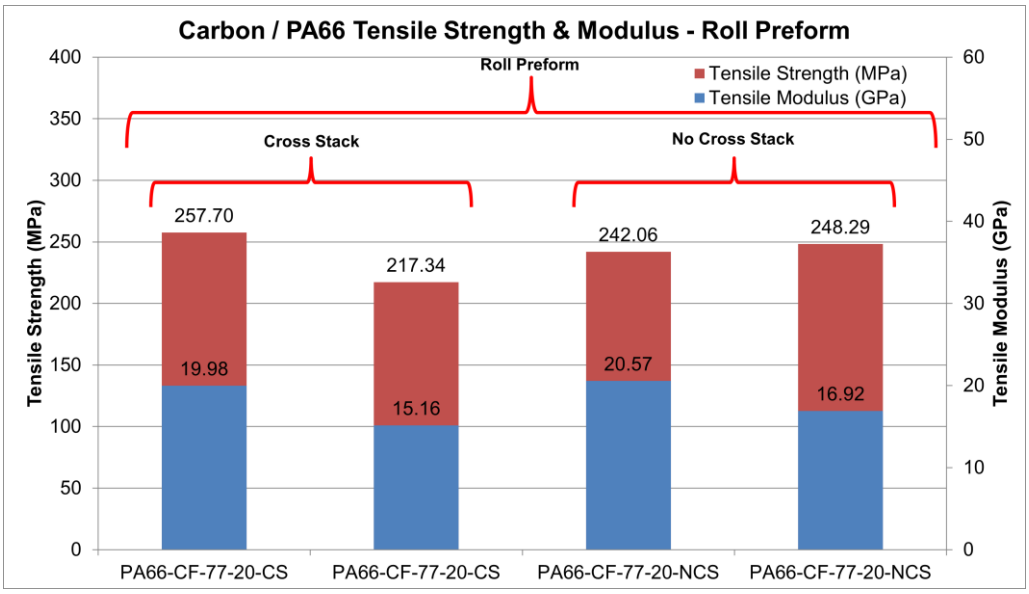

Figure 5. Comprehensive summary of tensile strength and tensile modulus for 'roll' form C/PA66.

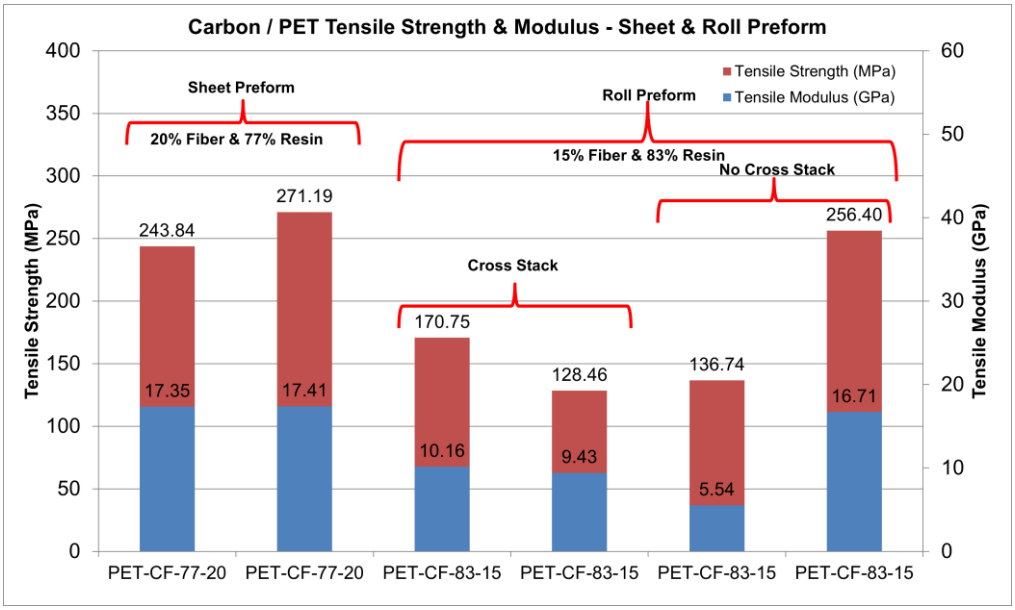

Figure 6. Comprehensive summary of tensile strength and tensile modulus for 'roll' and 'sheet' form C/PET.

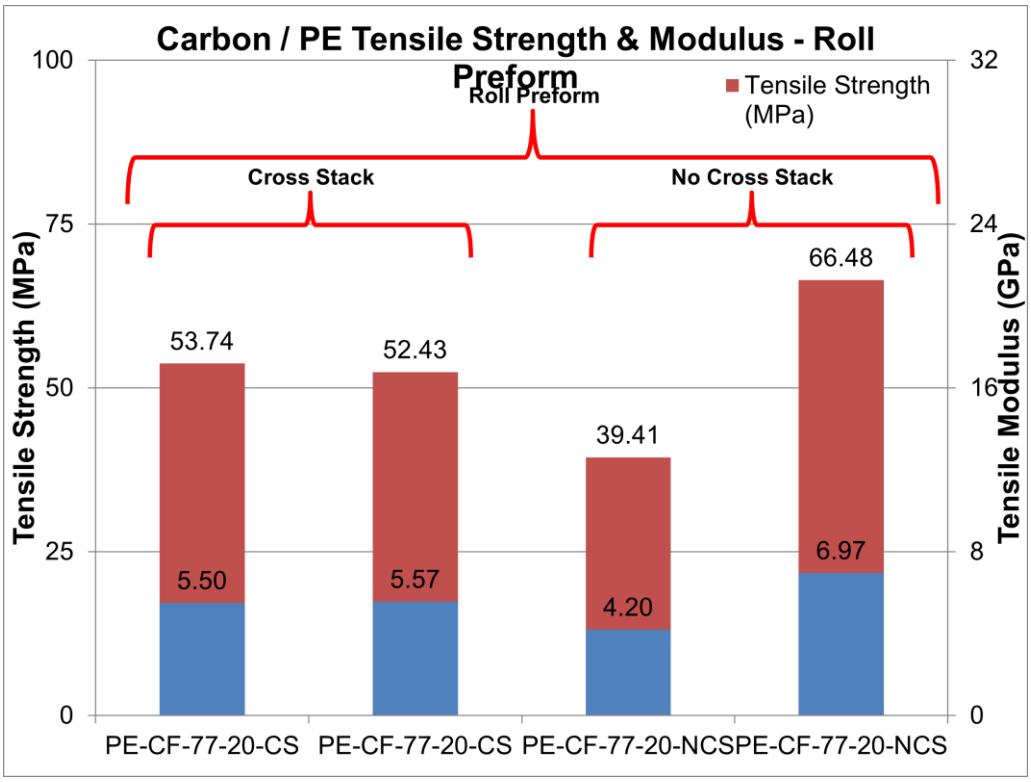

Figure 7. Comprehensive summary of tensile strength and tensile modulus for 'roll' form no stack and cross-stack—C/PE.

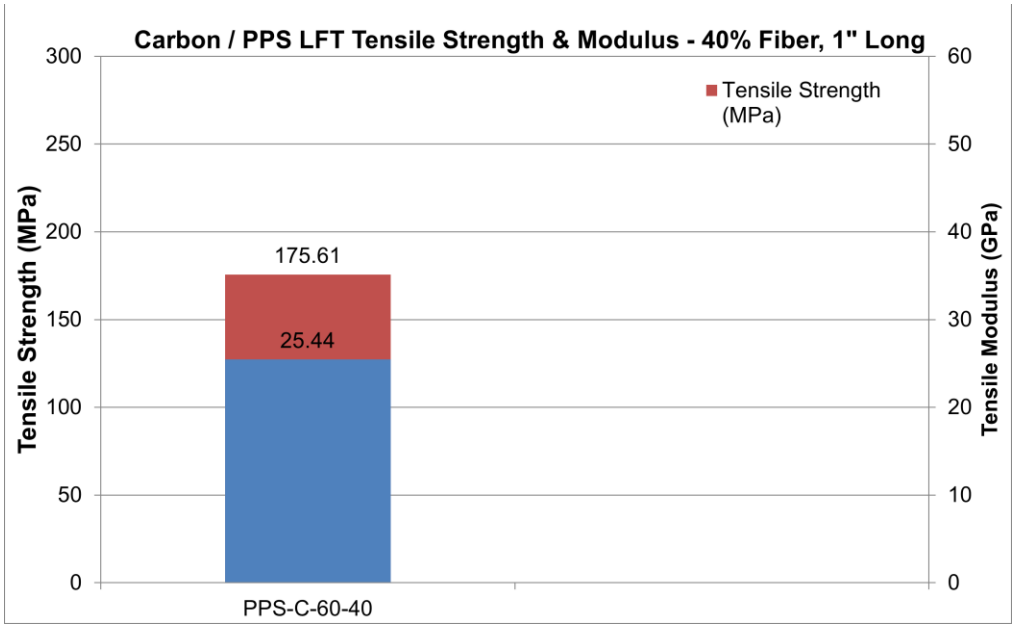

Figure 8. Benchmark tensile strength and tensile modulus for LFT C/PPS 40 wt% CF.

6. Processing Studies

Optimal processing results were obtained from panels produced with tool temperature at 500 °F. The panels processed at 250–265 F tool temperature exhibited voids, as seen in Figure 1a,b. All panels used for testing were, hence, processed at 500 °F tool temperature. Several processing routes were attempted from the rCF mats.

(a) Compression molding of the preform in matched metal tool produced composite plates. The compression molding of the PA66 rCF mats was conducted to different consoli-

dation pressures. This helped understand process temperature–pressure–microstructure relationships. The fully consolidated panels were used for mechanical testing/data generation; (b) compression molding of C/PA66 panels followed by pre-heating the consolidated panel and subsequently subjecting the heated panel to single-diaphragm thermoform (SDF), and (c) pre-heating the C/PA66 mats without compression molding (hence, a less stiff mat) and subjecting it to SDF.

6.1. Single-Diaphragm Forming of Pre-Consolidated Panel

The purpose of this study was to evaluate the formability of the mat(s) in terms of draw. PA66/CF/78/20 was consolidated using the 300 × 300 mm^2 tool for a 2.5 mm thick panel at 500 °F and 6.895 MPa (1000 psi). The consolidated panel (blank) was then re-heated in a convection oven for approximately 5 min at 490–500 °F. There was very little sag (if any) evident. A toy car mold (250 × 100 × 125 mm^3) was used as a tool to thermoform the consolidated blank. The blank exhibited some discoloration inside the oven. The blank was unable to soften and did not reach the melt temperature without degradation. As such, one atmosphere vacuum was used to form the part. The consolidated blank failed catastrophically during forming, as seen in Figure 9.

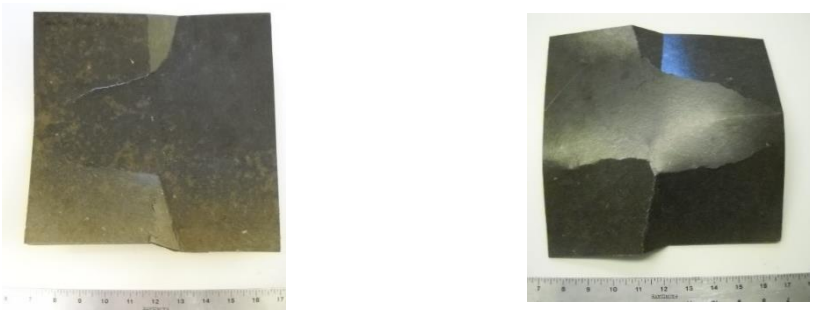

(**a**) (**b**)

Figure 9. Pre-consolidated blank (after heating and thermoforming). Sample—PA66/CF/78/20, 5 layers of preform; (**a**) exposed side in oven shows much yellowing; (**b**) non-exposed side shows less yellowing.

The pre-consolidated C/PA66 plate did not sag, hence, the plate was stiff when transferred from the oven to the forming station. Due to this, it appears that well-consolidated plates possess limited ability to form to shape, resulting in cracking in the C/PA66 resin. It appears that heating of the preforms must be done in a vacuum oven/inert condition to prevent discoloration (yellowing). Whether the yellowing is from moisture remains unclear. To find the cause for discoloration when the PA66/CF is heated in an oven, the preform was heated under vacuum or inert atmosphere to determine if discoloration occurs due to the presence of air, as shown in Table 15.

Table 15. Mats produced via different processing routes.

Sample Variants	Preform Type	Compression Molding	Single Diaphragm	Oven Compression Molding
Sample-PA66-CF-68-30	Sheets of 14″ × 14″	Yes	Yes	Yes
Sample-PA66-CF-78-20	Sheets of 14″ × 14″	Yes	Yes	No
Sample-PA66-CF-88-10	Sheets of 14″ × 14″	Yes	No	No
Sample-PA66-CF-77-20	Roll	Yes	No	
Sample-PE-CF-78-20	Roll	Yes	Yes	Yes

6.2. Compression Molding—External Heating (Heating the Preforms in a Convection Oven)

Two layers of PA66/CF/88/10 were placed in a convection oven at 500 °F for 5 min. A heated mold (with oil heating up to 350 °F) was used to compression mold the heated preforms. The blanks exhibited some discoloration inside the oven, see Figure 10a,b. Only the top layers of the preform became discolored due to heat. The bottom did not reach the processing temperature, nor did it discolor. Further, 1000 psi of positive pressure was applied on the tool.

(**a**) Exposed side (in oven) (**b**) non-exposed side

Figure 10. Heated preforms after compression molding.

6.3. Single-Diaphragm Forming—PE/CF

One layer of PE-CF-78-20 was heated in an oven at 350 F for 5–6 min. The heated preform was transferred to the mold and subjected to one atmosphere of vacuum. The material formed well without any discoloration, see Figure 11.

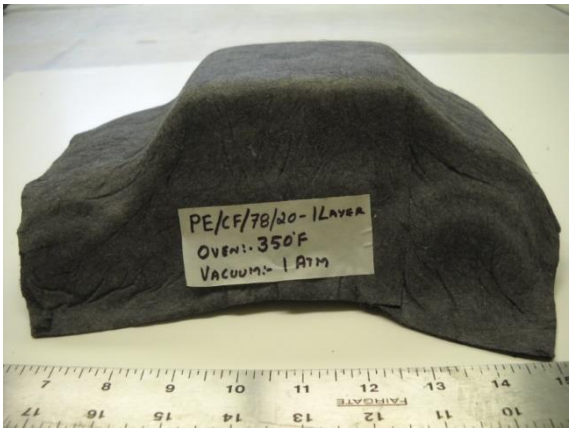

Figure 11. Forming via SDF exhibited optimal draw and consolidation.

6.4. Compression Molding—External Heating (Heating the Preforms in a Convection Oven)

Two layers of PE/CF/78/20 were heated in a convection oven at 400 °F for 10 min. An in-house heated mold (with oil heating at 250 °F) was used as a tool to compression mold the heated preforms. There was "no" discoloration of the blank inside the oven, see Figure 12a,b. Subsequently, 6.895 MPa (1000 psi) of positive pressure was applied on the tool.

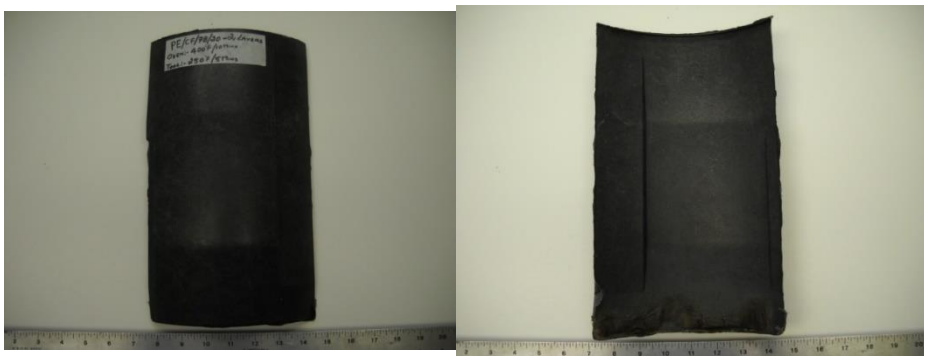

(**a**) Top side (**b**) Back side

Figure 12. Forming of shell shape through external heating and compression molding.

6.5. Discussion on Heating the Mats

Since the mats have significant open porosity and air (before consolidation), getting the mats to attain their processing temperature is important. Hence, pre-heating brings the mats to a uniform temperature and assists with the processing. It was observed that prior to consolidation, uniform heating of the mats, either in infrared oven or via contact heating in the closed-cavity, brings the mats to a processable condition. While the mechanical properties are more a function of optimal temperature and consolidation pressure, the efficient way to get to these conditions is via pre-heating to minimize time in the press (hence, higher process efficiency).

7. Conclusions

rCF WL mats were successfully produced in three resin types—PA66, PE and PET. The processing method had significant influence on properties. The 'sheet' form exhibited random/quasi-isotropic properties while the properties in the 'roll' form were guided by the preferred fiber orientation. The tensile strength and modulus were 80–120% higher on average in the 'roll' form compared to the 'sheet' form.

The tensile strength and modulus of the 77 wt% resin, ~20 wt% fiber mats ranked as C/PA66 > C/PET > C/PE guided by the resin properties. Some variants, such as C/PE 20 wt% carbon fiber, had higher anisotropy, i.e., they were more sensitive for the cross-stack versus no-stack, while in some variants, the fiber entanglement seems to minimize the influence of fiber orientation, i.e., differences in properties in the no-stack versus cross-stack were less discernable.

The impact response of the rCF mats indicated the best performance came from C/PA66, while the energy absorbed by C/PE is assumed to be the highest, due to the weaker bonding between C and PE; as evident from the strength and modulus, this helps with energy absorption.

For PA66-CF, pre-drying was an important step as it influenced the properties by a factor of 2 or greater; pre-dried mats performed higher. The formability of pre-consolidated WL composites was poor due to high stiffness. Matched metal die provided the best forming of the WL mats for all the resin systems. The material loses heat rapidly, hence, the forming must be conducted immediately to pre-heating. The best formability was achieved in the PE-CF mats.

with the DOE Public Access Plan (http://energy.gov/downloads/doe-public-access-plan) (accessed on 15 June 2022).

Author Contributions: Conceptualization, M.J. and U.V.; methodology, U.V. and H.G.; validation, M.J., K.G., M.T. and U.V.; formal analysis, U.V.; investigation, U.V. and H.G.; resources, K.G., M.J. and M.T.; data curation, U.V.; writing—original draft preparation, M.J., K.G. and M.T.; writing—review and editing, supervision, U.V. and M.J.; project administration, M.J.; funding acquisition, M.J. All authors have read and agreed to the published version of the manuscript.

Funding: This study was supported by the Department of Energy for the project entitled Low Cost Carbon Fiber Composites for Lightweight Vehicle Parts, Materials Innovation Technologies, LLC, Contract #DOE-EE0004539, US DOE SBIR Phase III.

Institutional Review Board Statement: Not applicable.

Informed Consent Statement: Not applicable.

Data Availability Statement: Not applicable.

Acknowledgments: The discussions with the Institute for Advanced Composites Manufacturing Innovation (IACMI)—The Composites regarding light-weighting technologies and recycling carbon fiber materials is gratefully acknowledged. IACMI was funded in part by the Office of Energy Efficiency and Renewable Energy (EERE), U.S. Department of Energy, under Award Number DE-EE0006926.

Conflicts of Interest: The authors declare no conflict of interest.

References

1. Bledzki, A.K.; Seidlitz, H.; Goracy, K.; Urbaniak, M.; Rösch, J.J. Recycling of Carbon Fiber Reinforced Composite Polymers—Review—Part 1: Volume of Production, Recycling Technologies, Legislative Aspects. *Polymers* **2021**, *13*, 300. [CrossRef] [PubMed]
2. Bledzki, A.K.; Seidlitz, H.; Krenz, J.; Goracy, K.; Urbaniak, M.; Rösch, J.J. Recycling of Carbon Fiber Reinforced Composite Polymers—Review—Part 2: Recovery and Application of Recycled Carbon Fibers. *Polymers* **2020**, *12*, 3003. [CrossRef] [PubMed]
3. BMW i Production CFRP Wackersdorf: Carbon Fiber Recycling Material for the Use in the BMW i3, e.g., the Roof of the BMW i3. 2013. Available online: www.press.bmwgroup.com/global/photo/detail/P90125888 (accessed on 20 May 2020).
4. The State of Recycled Carbon Fiber. 2019. Available online: www.compositesworld.com/articles/the-state-of-recycled-carbon-fiber (accessed on 26 July 2020).
5. Technology Roadmap, IACMI-The Composites Institute. Available online: www.iacmi.org (accessed on 22 April 2022).
6. Closing the Loop, Carbon Conversions. Available online: https://carbonconversions.com/ (accessed on 17 June 2022).
7. Wöllinga, J.; Schmiega, M.; Manisa, F.; Drechslerb, K. Nonwovens from recycled carbon fibres—Comparison of processing technologies. In Proceedings of the 1st Cirp Conference on Composite Materials Parts Manufacturing, Procedia CIRP, Karlsruhe, Germany, 8–9 June 2017; Volume 66, pp. 271–276. [CrossRef]
8. Song, Y.; Gandhi, U.; Sekito, T.; Vaidya, U.K.; Hsu, J.; Yang, A.; Osswald, T. A Novel CAE Method for Compression Molding Simulation of Carbon Fiber-Reinforced Thermoplastic Composite Sheet Materials. *J. Compos. Sci.* **2018**, *2*, 33. [CrossRef]
9. Selezneva, M.; Lessard, L. Characterization of mechanical properties of randomly oriented strand thermoplastic composites. *J. Compos. Mater.* **2016**, *50*, 2833–2851. [CrossRef]
10. Thomason, J. The influence of fibre length and concentration on the properties of glass fibre reinforced polypropylene: 5. Injection moulded long and short fibre PP. *Compos. Part A Appl. Sci. Manuf.* **2002**, *33*, 1641–1652. [CrossRef]
11. Vaidya, U.K. *Composites for Automotive, Mass Transit and Heavy Truck*; DesTech Publishers: Lancaster, PA, USA, 2010.
12. Stoeffler, K.; Andjelic, S.; Legros, N.; Roberge, J.; Schougaard, S.B. Polyphenylene sulfide (PPS) composites reinforced with recycled carbon fiber. *Compos. Sci. Technol.* **2013**, *84*, 65–71. [CrossRef]
13. Borkar, A.; Hendlmeier, A.; Simon, Z.; Randall, J.D.; Stojcevski, F.; Henderson, L.C. A comparison of mechanical properties of recycled high-density polyethylene/waste carbon fiber via injection molding and 3D printing. *Polym. Compos.* **2022**, *43*, 2408–2418. [CrossRef]
14. Baek, Y.-M.; Shin, P.-S.; Kim, J.-H.; Park, H.-S.; Kwon, D.-J.; DeVries, K.L.; Park, J.-M. Investigation of Interfacial and Mechanical Properties of Various Thermally-Recycled Carbon Fibers/Recycled PET Composites. *Fibers Polym.* **2018**, *19*, 1767–1775. [CrossRef]
15. Hemamalini, T.; Dev, V.R.G. Wet Laying Nonwoven Using Natural Cellulosic Fibers and Their Blends: Process and Technical Applications. A Review. *J. Nat. Fibers* **2019**, *18*, 1823–1833. [CrossRef]
16. Melani, L.; Kim, H.-J. The surface softness and mechanical properties of wood pulp–lyocell wet-laid nonwoven fabric. *J. Text. Inst.* **2020**, *112*, 1191–1198. [CrossRef]
17. Ghossein, H.; Hassen, A.A.; Kim, S.; Ault, J.; Vaidya, U.K. Characterization of Mechanical Performance of Composites Fabricated Using Innovative Carbon Fiber Wet-laid Process. *J. Compos. Sci.* **2020**, *4*, 124. [CrossRef]

18. Yan, X.; Wang, X.; Yang, J.; Zhao, G. Optimization of process parameters of recycled carbon fiber-reinforced thermoplastic prepared by the wet-laid hybrid nonwoven process. *Text. Res. J.* **2021**, *91*, 1565–1577. [CrossRef]
19. Ghossein, H.K. Novel Wet-Laid Nonwoven Carbon Fiber Mats and Their Composites. Ph.D. Thesis, University of Tennessee, Knoxville, TN, USA, 2018.
20. Barnett, P.R.; Young, S.A.; Chawla, V.; Foster, D.M.; Penumadu, D. Thermo-mechanical characterization of discontinuous recycled/repurposed carbon fiber reinforced thermoplastic organosheet composites. *J. Compos. Mater.* **2021**, *55*, 3409–3423. [CrossRef]
21. Erland, S.; Stevens, H.; Savage, L. The re-manufacture and repairability of poly(ether ether ketone) discontinuous carbon fibre composites. *Polym. Int.* **2021**, *70*, 1118–1127. [CrossRef]
22. Brahma, S.; Pillay, S.; Ning, H. Comparison and characterization of discontinuous carbon fiber liquid-molded nylon to hydroentanglement/ compression-molded composites. *J. Thermoplast. Compos. Mater.* **2020**, *33*, 1078–1093. [CrossRef]
23. Yeole, P.; Hassen, A.A.; Vaidya, U.K. The effect of flocculent and dispersants on wet–laid process for recycled glass fiber/PA6 composite. *Polym. Polym. Compos.* **2018**, *26*, 259–269. [CrossRef]
24. Kore, S.; Spencer, R.; Ghossein, H.; Slaven, L.; Knight, D.; Unser, J.; Vaidya, U. Performance of hybridized bamboo-carbon fiber reinforced polypropylene composites processed using wet-laid technique. *Compos. Part C Open Access* **2021**, *6*, 100185. [CrossRef]